Electronic Supplementary Material (ESI) for Materials Horizons.

Supporting Information

Significant Increase of Photoresponse Range and Conductivity for a Chalcogenide Semiconductor by Viologen Coating through Charge Transfer

Tian-Tian Song, Wei-Qiang Huang, Kai-Bin Jiang, Wen-Fa Chen, Yu Zhou, Hong-Yi Bian, Ming-Sheng Wang* and Guo-Cong Guo*

Table of Contents

1. Experimental Procedures

1.1 Characterization

Elemental Analysis: Analysis of C and N elemental in $KGaS_2$ and **MV@$KGaS_2$** were got from an Elementar Vario EL III microanalyzer.

PXRD: PXRD patterns of the samples were collected on Rikagu Miniflex 600 Benchtop X-ray diffraction instrument.

SEM: SEM images were recorded on a Zeiss Sigma 300 field emission scanning electron microscope. The used accelerating voltage is 3 kV.

NMR: ^1H NMR spectra were recorded on Bruker AVANCE III 400MHz spectrometers.

UV/Vis/NIR Absorption: UV/Vis/NIR absorption spectra were recorded on a PerkinElmer Lambda 900 UV/vis/NIR spectrophotometer equipped with an integrating sphere using $BaSO_4$ as the reference.

Raman: Raman spectra were collected at room temperature using a Renishaw invia-Reflex Micro-Raman Spectroscopy system equipped with a 633 nm laser.

XPS: XPS measurements were performed using an ESCALAB 250Xi spectrometer (Thermo Fisher Co., Ltd.), monochromatic Al-Kα radiation (E = 1486.2 eV) was used in combination with Ar ion beam sputter etching to remove the surface coating (tantalum pentoxide was used as a reference for XPS etch depth). All peak energies were referenced to the adventitious C1s, C–C peak at 284.8 eV for calibration purposes.

EPR Test: EPR spectra were measured by a Bruker-BioSpin E500 spectrometer at room temperature.

Electrical Test: All electrical measurements were performed on Keithley 4200-SCS semiconductor parameter analyzers.

PL: PL decay curves of $KGaS_2$ and **MV@$KGaS_2$** were measured through a FLS 1000 fluorescence spectrophotometer under a 360 nm laser excitation (Maximum Average Power 5mW).

UPS: UPS measurements were performed using an Thermo Fisher Nexsa spectrometer.

Hall Effect: Hall coefficients and carrier mobilities were characterized in van der Pauw geometries[3] using a commercial Hall system (HMS-3000).

1.2 Light source

We used a series of semiconductor lasers for the UV-vis (375, 420, 520, 635 nm) regions (Changchun New Industries Optoelectronics Tech Co., Ltd.) and a laser power meter (with probe, CNI Laser. Changchun New Industries Optoelectronics Tech Co., Ltd.) to measure the photoresponsive behaviors of $KGaS_2$ and **MV@$KGaS_2$**.

1.3 Materials

All chemicals are commercially sourced and used without additional purification. Alkaline earth metals Ba (99.99%, Aladdin), Mg (99.99%, Aladdin), Ga (99.99%, Aladdin), S (99%, Sinopharm Chemical Reagents Co Ltd), KCl (99.5%, Tianjin Kemiou Chemical Reagent Co., Ltd.), 4,4'-biphyridine (98%, Bide Pharmatech Ltd.), Chloroacetic acid (99%，TCI), Ethanol (AR, Sinopharm Chemical Reagents Co Ltd), Dichloromethane (AR, Sinopharm Chemical Reagents Co Ltd), Acetonitrile (AR, Sinopharm Chemical Reagents Co Ltd), *N*,*N*-dimethylformamide (DMF, AR, Sinopharm Chemical Reagents Co., Ltd.), Milli Q Ultra Pure Water (18.2 MΩ·cm) Formulation.

1.4 First-principles calculation

All calculations were performed with periodic DFT using the Gaussian and plane waves (GPW) method implemented in CP2K's Quickstep module[1]. The explorative studies of these structures were performed using the molecularly optimized basis set DZVP-MOLOPT-SR-GTH for each atom with a Goedecker-Teter-Hutter (GTH) pseudopotential[2]. The calculations were conducted using the generalized gradient approximation and the Perdew-Burke-Ernzerhof (PBE) functional[3] with D3 (BJ) correction[4]. An energy convergence for the self-consistent field (SCF) calculation was set to 5 × 10−6 Hartree. An energy cutoff of 350 Ry was used throughout the calculations. Vacuum spacing larger than 15 Å is introduced to avoid artificial interaction between the periodic images along the z-direction. The input file was generated by Multiwfn software[5].

1.5 Conductivity calculation

The resistivity (ρ) values for $KGaS_2$ and **MV@KGaS$_2$** were obtained from the equation

$$\rho = R \frac{S}{L} \#(S1)$$

where R is the resistance, S is the contact area between the probe and the sample, and L is the length. The R values for $KGaS_2$ and **MV@KGaS$_2$** are obtained from the linear region of the I-V curve over a bias range of ±10 V. Thus, we further obtained the conductivity (σ) values[6].

1.6 Carrier mobility calculation

To measure the Hall effect of the material, quartz glass (10×10 mm^2) was used as the substrate, and before preparing the material, the quartz glass needs to be cleaned first. The cleaning steps are as follows: the quartz glass was ultrasonically cleaned in acetone, DMF, anhydrous ethanol, and deionized water sequentially for 30 min each time, and the cleaning process was repeated three times, and then naturally dried and set aside. The test samples were prepared by weighing 20 mg of $KGaS_2$ and **MV@KGaS$_2$** powder samples with a particle size of 0.15 mm dispersed in 5 mL of ethanol and spin-coated on the knotted quartz glass. To obtain the Ohmic contacts, silver wires were placed in contact with the samples using silver conductive adhesive paste. The samples were measured in a magnetic field of 0.553 T perpendicular to the sample plane. The Hall coefficient (R_H) and carrier mobility (μ) were determined from the measurement of the Hall voltage (V_H) according to the basic physical principles of the Hall effect[7]

$$R_H = (d/B)\left(V_H/I\right) \#(S2)$$

$$n = 1/\left(\left|R_H\right|q\right) \#(S3)$$

$$\mu = \left|V_H\right|/I \frac{B}{} \#(S4)$$

$$\mu = 1/q \frac{R_H}{} \#(S5)$$

where d is the sample thickness, I is the current, B is the magnetic field, q is the electron charge (1.602×10^{-19} C), n is the carrier concentration, and R_H is the Hall factor. In addition, the positive and negative R_H indicate which carriers dominate the conductive behavior, being negative for n-type semiconductors (electrons) and positive for p-type semiconductors (holes).

1.7 Preparation of $KGaS_2$

For the preparation of $KGaS_2$, based on the methods given in the literature[8], reactants of Mg (0.42 mmol), Ba (0.42 mmol), Ga (2.07 mmol), S (4.05 mmol), KCl (2.07 mmol), were mixed and respectively loaded into silica tubes inside an Ar-filled glove box. Then the ampules were flame-sealed under 10^{-3} Pa and placed in a temperature-controlled furnace with the following heating process: firstly, heated to 400 °C rate of 50 °C/h and held there for 20 h, then heated to 850 °C at a rate of 30 °C/h and kept at that temperature for 96 h. Finally, the furnace was slowly cooled down to room temperature at a rate of 5 °C/h. Single-crystal was obtained after washing products in deionized water. Selected individual crystal was analyzed on energy dispersive analyses X-ray spectroscopy (EDS).

1.8 Preparation of MV

Synthesis is based on the methods given in the literature[9]. A precipitate was formed by heating *4,4'*-bipyridine (5 g, 32.0 mmol) and chloroacetic acid (8.17 g, 86.0 mmol) in acetonitrile (30.0 mL) to reflux at 88°C for 24 hours. After cooling to room temperature, the precipitate formed was washed with warm DMF (20 mL), dichloromethane (10 mL), acetonitrile and subsequently dried to give a white solid product.

1.9 Preparation of $MV@KGaS_2$

The well-shaped $KGaS_2$ crystals obtained from **1.7** preparation without cracks were picked with a silver needle and placed on a clean slide. Dissolve 520 mg of MV in 10 ml of deionized water to prepare solutions with a concentration of 0.2 mol/L, respectively. After 30 min of sonication, the solution was filtered through a 0.45 μm syringe filter and set aside. The prepared 0.2 mol/L MV solution was slowly added dropwise to the crystals. Then the slides were placed on the Petri dishes and the Petri dishes were wrapped with cling film that was perforated by a needle. After standing for 6h, the material was carefully removed with forceps and then washed with water and ethanol three times, respectively, and left to dry to obtain orange-red flake material.

2. Supplementary Figures

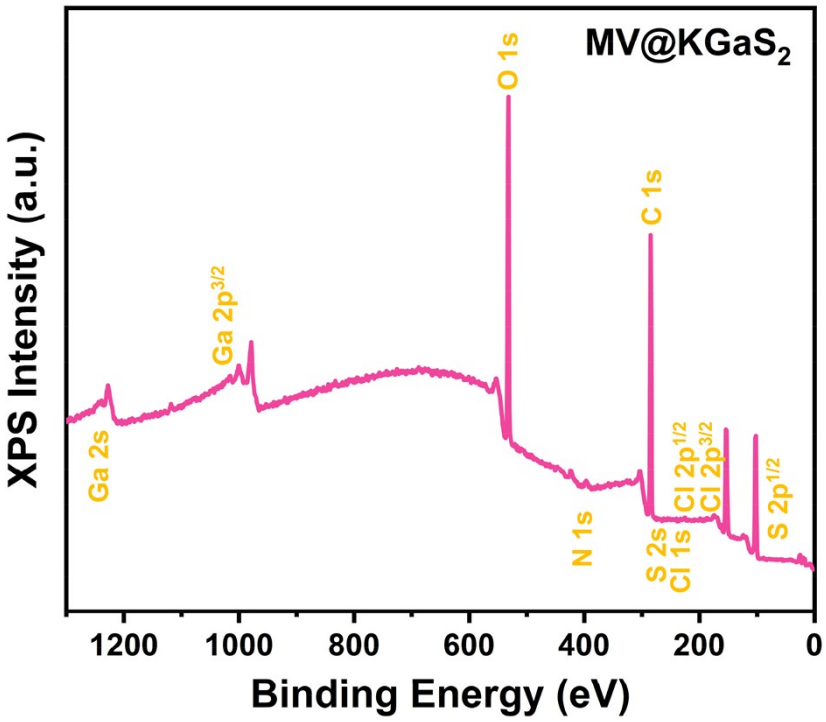

Figure S1. XPS survey spectra of **MV@KGaS$_2$**.

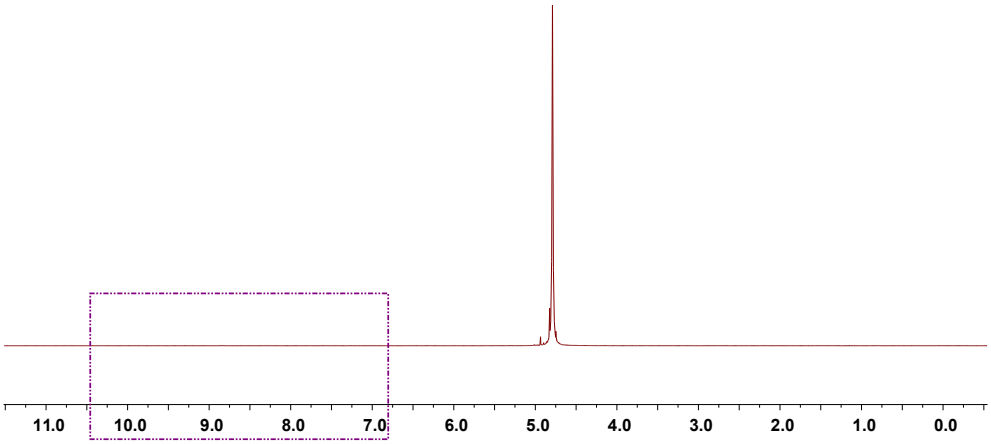

Figure S2. ^{1}H NMR pattern of **MV@KGaS$_2$** (D_2O).

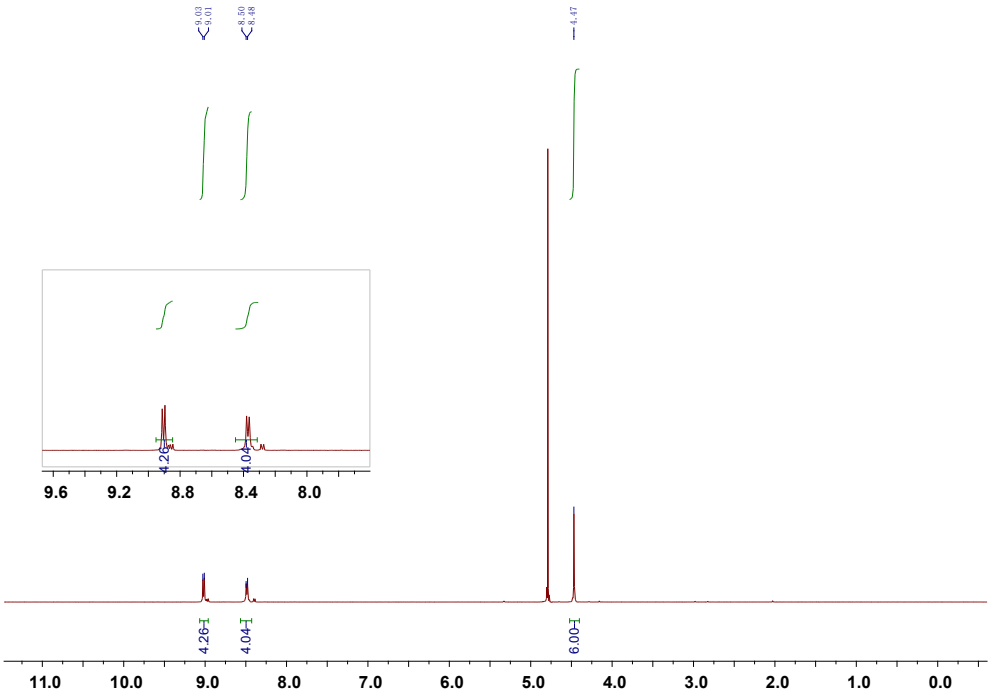

Figure S3. ^{1}H NMR pattern of 0.3 mg MV (D_2O).

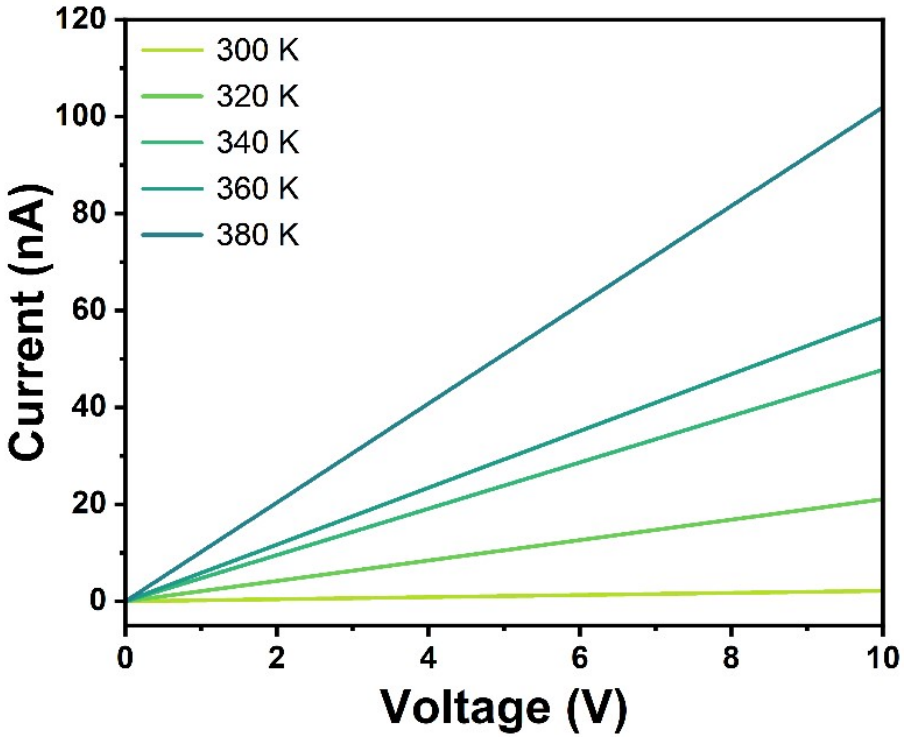

Figure S4. The temperature dependent *I*–*V* curves of $KGaS_2$ single crystal device.

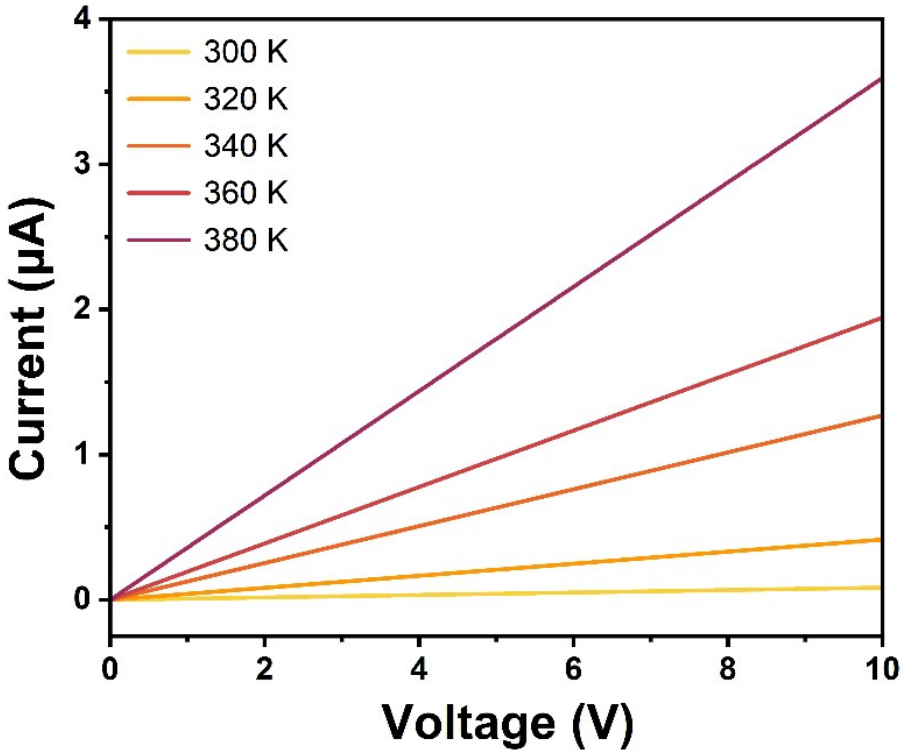

Figure S5. The temperature dependent *I*–*V* curves of **MV@$KGaS_2$** single crystal device.

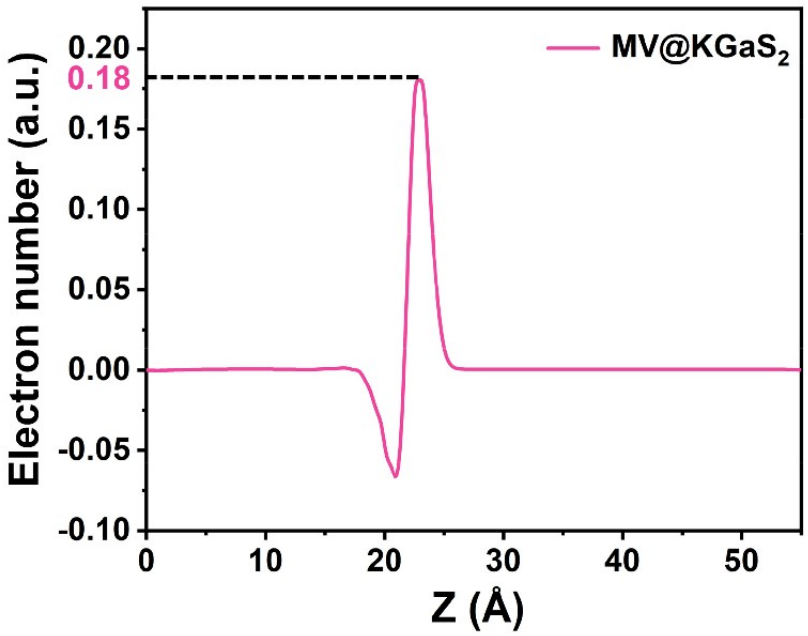

Figure S6. The number of electrons transferred in the charge transfer interaction between MV and $KGaS_2$.

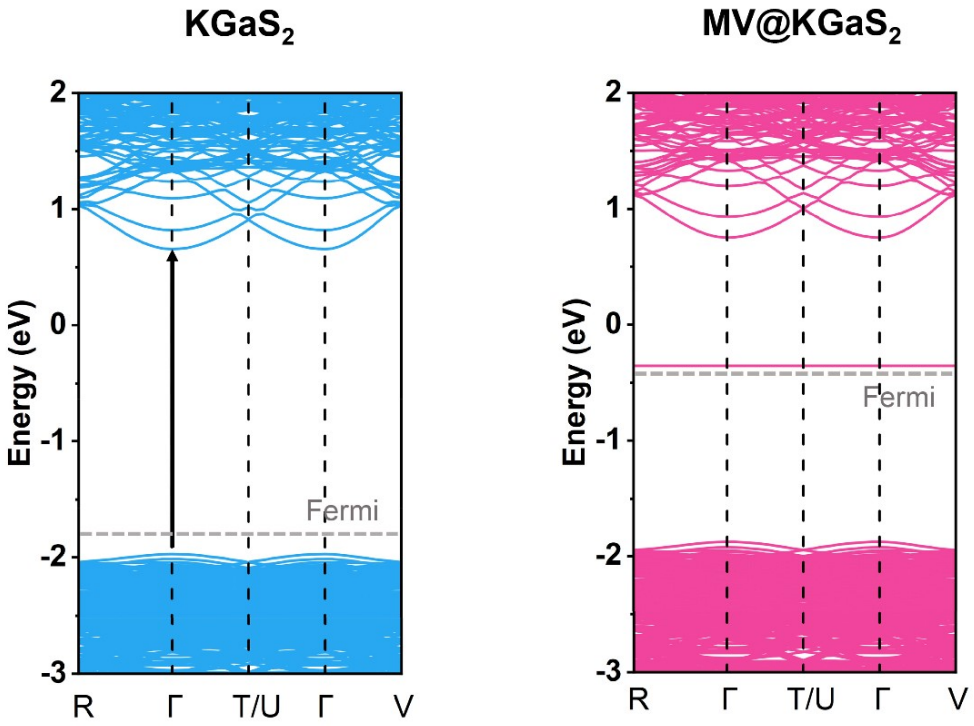

Figure S7. Band structures of the $KGaS_2$ (the left) and **MV@KGaS$_2$** (the right).

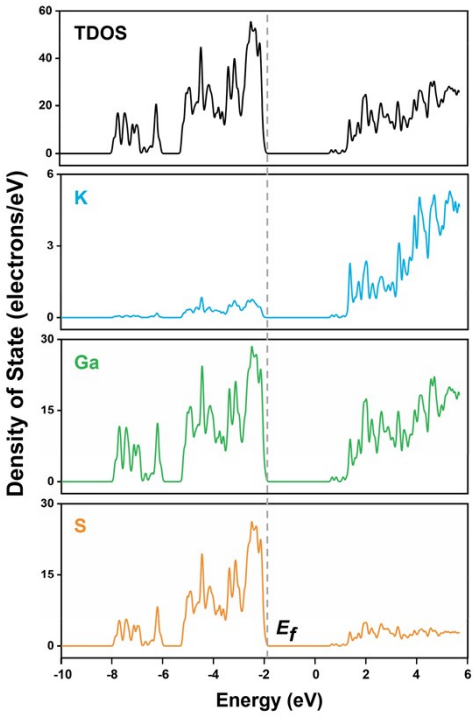

Figure S8. Total and partial density of states (TDOS and PDOS) of $KGaS_2$.

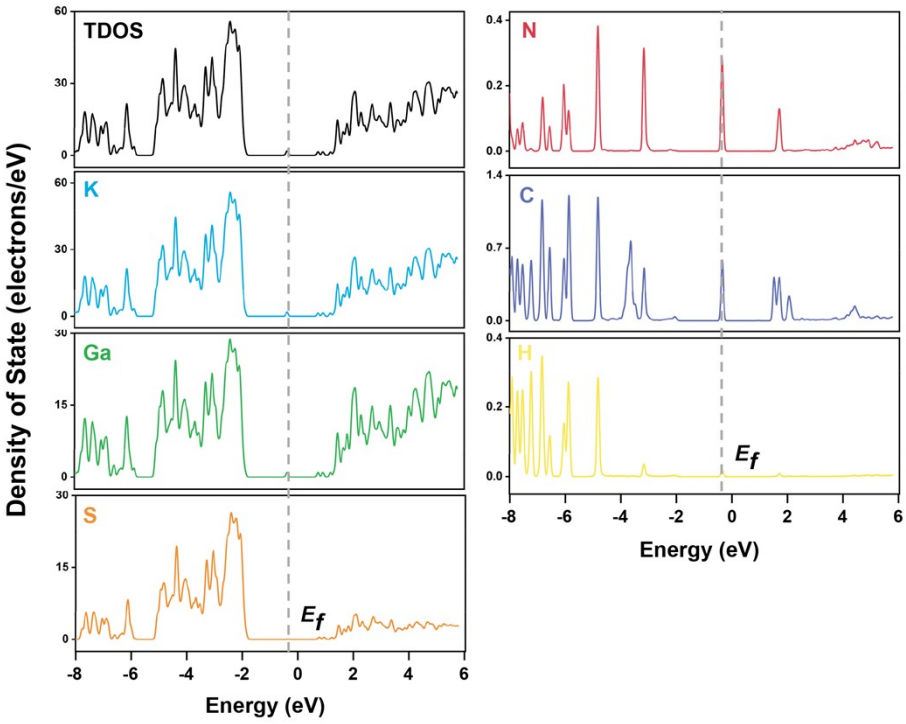

Figure S9. Total and partial density of states (TDOS and PDOS) of **MV@$KGaS_2$**.

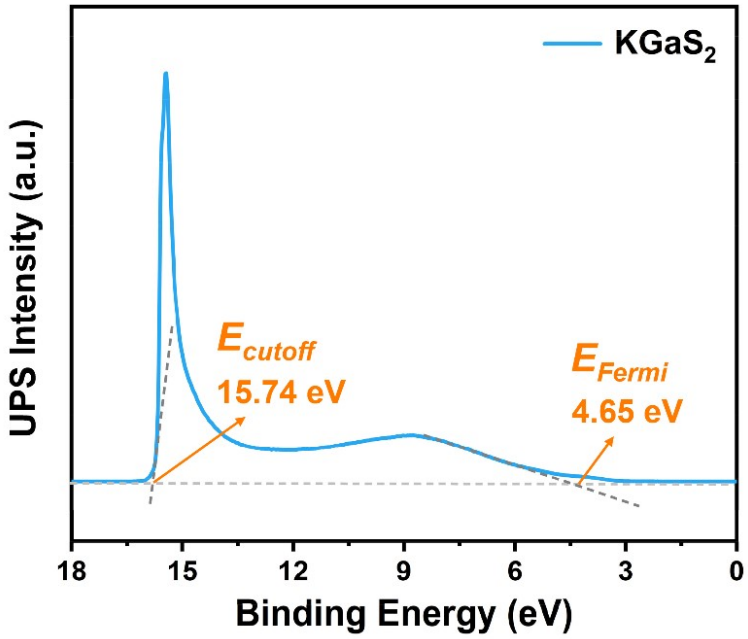

Figure S10. UPS spectrum of the $KGaS_2$. According to the linear intersection method, the E_{VB} of the $KGaS_2$ was calculated to be –10.13 eV (vs. vacuum; the excitation energy *hv* of the He I Source Gun is 21.22 eV[10]) from $hv+E_{Fermi}–E_{cutoff}$.

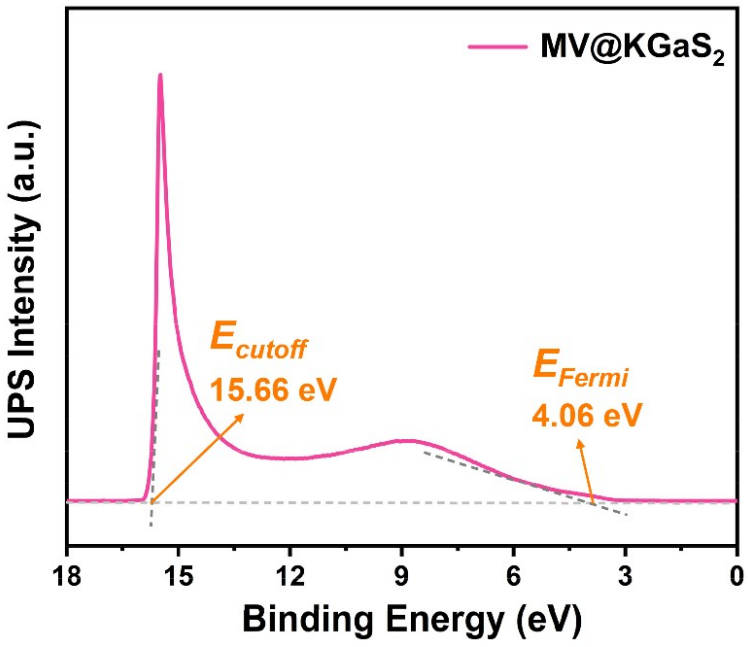

Figure S11. UPS spectrum of the MV@$KGaS_2$. According to the linear intersection method, the E_{VB} of the **MV@$KGaS_2$** was calculated to be –9.62 eV (vs. vacuum; the excitation energy *hv* of the He I Source Gun is 21.22 eV) from $hv+E_{Fermi}–E_{cutoff}$.

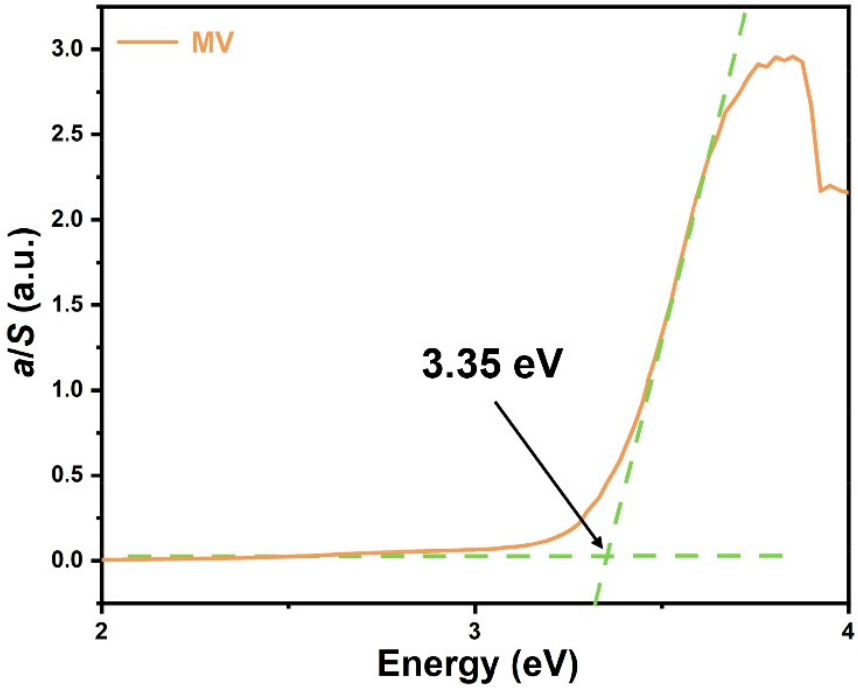

Figure S12. Kubelka–Munk plot based on the diffuse reflectance data of the MV.

3. References

[1] a) T. D. Kuhne, M. Iannuzzi, M. Del Ben, V. V. Rybkin, P. Seewald, F. Stein, T. Laino, R. Z. Khaliullin, O. Schutt, F. Schiffmann, D. Golze, J. Wilhelm, S. Chulkov, M. H. Bani-Hashemian, V. Weber, U. Borstnik, M. Taillefumier, A. S. Jakobovits, A. Lazzaro, H. Pabst, T. Muller, R. Schade, M. Guidon, S. Andermatt, N. Holmberg, G. K. Schenter, A. Hehn, A. Bussy, F. Belleflamme, G. Tabacchi, A. Gloss, M. Lass, I. Bethune, C. J. Mundy, C. Plessl, M. Watkins, J. VandeVondele, M. Krack and J. Hutter, *J. Chem. Phys.,* 2020, **152**, 194103; b) J. VandeVondele, M. Krack, F. Mohamed, M. Parrinello, T. Chassaing and J. Hutter, *Comput Phys Commun*., 2005, **167**, 103-128.

[2] a) M. Krack, *Theor Chem Acc.* **2005**, *114*, 145-152; b) J. VandeVondele and J. Hutter, *J. Chem. Phys.,* 2007, **127**, 114105; c) B. G. Lippert, J. H. Parrinello, Michele, *Mol Phys.* **2010**, *92*, 477-488; d) C. Hartwigsen, S. Goedecker and J. Hutter, *Phys. Rev.,* 1998, **58**, 3641-3662.

[3] J. P. Perdew, K. Burke and M. Ernzerhof, *Phys. Rev. Lett.,* 1996, **77**, 3865-3868.

[4] S. Grimme, S. Ehrlich and L. Goerigk, *J. Comput. Chem.,* 2011, **32**, 1456-1465.

[5] T. Lu and F. Chen, *J. Comput. Chem.,* 2012, **33**, 580-592.

[6] C. Sun, G. Xu, X. M. Jiang, G. E. Wang, P. Y. Guo, M. S. Wang and G. C. Guo, *J. Am. Chem. Soc.,* 2018, **140**, 2805-2811.

[7] M. Wang, M. Wang, H. H. Lin, M. Ballabio, H. Zhong, M. Bonn, S. Zhou, T. Heine, E. Canovas, R. Dong and X. Feng, *J. Am. Chem. Soc.,* 2020, **142**, 21622-21627.

[8] a) S. Shim, W. B. Park, M. Kim, J. W. Lee, S. P. Singh and K. S. Sohn, *Inorg Chem.,* 2021, **60**, 6047-6056; b) V. Bikbaeva, O. Perez, N. Nesterenko and V. Valtchev, *Inorg. Chem. Front.,* 2022, **9**, 5181-5187; c) B. W. Liu, X. M. Jiang, H. Y. Zeng and G. C. Guo, *J. Am. Chem. Soc.,* 2020, **142**, 10641-10645.

[9] C. Sun, M. S. Wang, P. X. Li and G. C. Guo, *Angew. Chem. Int. Ed.,* 2017, **56**, 554-558.

[10] a) K. B. Jiang, W. Q. Huang, T. T. Song, P. X. Wu, W. F. Wang, Q. S. Chen, M. S. Wang and G. C. Guo, *Adv. Funct. Mater.,* 2023, 2304351.; b) D. Zhao, Y. Wang, C.-L. Dong, Y.-C. Huang, J. Chen, F. Xue, S. Shen and L. Guo, *Nat. Energy.,* 2021, **6**, 388-397.